JACS
JOURNAL OF THE AMERICAN CHEMICAL SOCIETY
pubs.acs.org/JACS
Article

Organocatalytic Asymmetric Multicomponent Cascade Reaction for the Synthesis of Contiguously Substituted Tetrahydronaphthols

Yidong Liu, Joseph A. Izzo, David McLeod, Sebastijan Ričko, Esben B. Svenningsen, Thomas B. Poulsen, and Karl Anker Jørgensen*

Cite This: *J. Am. Chem. Soc.* 2021, 143, 8208−8220

ABSTRACT: Isobenzopyrylium ions are unique, highly reactive, aromatic intermediates which are largely unexplored in asymmetric catalysis despite their high potential synthetic utility. In this study, an organocatalytic asymmetric multicomponent cascade via dienamine catalysis, involving a cycloaddition, a nucleophilic addition, and a ring-opening reaction, is disclosed. The reaction furnishes chiral tetrahydronaphthols containing four contiguous stereocenters in good to high yield, high diastereoselectivity (up to >20:1), and excellent enantioselectivity (93−98% ee). The obtained products are important synthetic intermediates, and it is demonstrated that they can be used for the generation of frameworks such as octahydrobenzo[*h*]isoquinoline and [2.2.2]octane scaffolds. Furthermore, mechanistic experiments involving oxygen-18-labeling studies and density functional theory calculations provide a vivid picture of the reaction mechanism. Finally, the bioactivity of 16 representative tetrahydronaphthol compounds has been evaluated in U-2OS cancer cells with some compounds showing a unique profile and a clear morphological change.

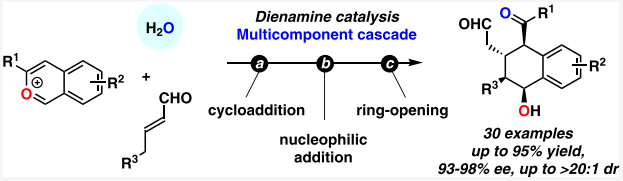

■ INTRODUCTION

Catalytic asymmetric cascade reactions exhibit distinct advantages in organic synthesis allowing for efficient enantioselective preparation of complex molecules.[1] Extensive efforts have been devoted to the development of novel reagents and the discovery of new activation modes for cascade reactions in asymmetric catalysis.[2]

Isobenzopyrylium ions have emerged as a unique type of reactive cyclic oxonium intermediates that have been shown to participate in a range of cascade reactions affording natural products and bioactive molecules.[3] In contrast, catalytic enantioselective cascade reactions with isobenzopyrylium ions remain significantly less developed.[4] The inherent challenges in their use arises from the high reactivity, aromatic planar structure, and the lack of a Lewis basic site needed for interactions with a potential catalyst. Nevertheless, innovative strategies to enable highly enantioselective transformations of isobenzopyrylium ions have been demonstrated.[5,6]

Transition metal−isobenzopyrylium intermediates, generated by cyclization of alkynyl carbonyl compounds, can be coupled either with electronically neutral chiral ligands, thereby affording a chiral electrophile, or combined with another transition-metal catalyst as a binary catalyst.[5a−d,i,k] By use of an asymmetric counteranion-directed catalysis (ACDC) strategy, metallo-isobenzopyrylium intermediates have been incorporated with chiral counteranions, and high enantioselectivities have been achieved through electrostatic interactions (Figure 1a).[5e−h,j]

Compared to the number of reported transition-metal-catalyzed asymmetric cascade reactions involving isobenzopyrylium ions, organocatalytic approaches are rare[6] even though asymmetric organocatalysis has been extensively applied in assembling chiral molecules.[7] To date, there are only two examples of catalytic asymmetric syntheses of dihydronaphthalenes utilizing the ACDC strategy reported independently by Sun and Schaus (Figure 1b).[6a,b] In these novel approaches, the catalytically generated chiral counteranion also works as the nucleophile.

To expand the scope and synthetic applicability of isobenzopyrylium ions, we present a novel catalytic regio-, diastereo-, and enantioselective multicomponent cascade via dienamine catalysis, consisting of first a cycloaddition, then a nucleophilic addition, and finally a ring-opening reaction affording contiguously substituted tetrahydronaphthols (Figure 1c). Through effective steric shielding by the organocatalyst, controlling the facial selectivity in the key carbon−carbon bond forming event involving the dienamine intermediate with the planar isobenzopyrylium ion, excellent stereoselectivity was obtained for the tetrahydronaphthol products. This important structural motif is central to many

Received: April 14, 2021
Published: May 24, 2021

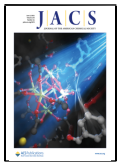

https://doi.org/10.1021/jacs.1c03923
J. Am. Chem. Soc. 2021, 143, 8208−8220

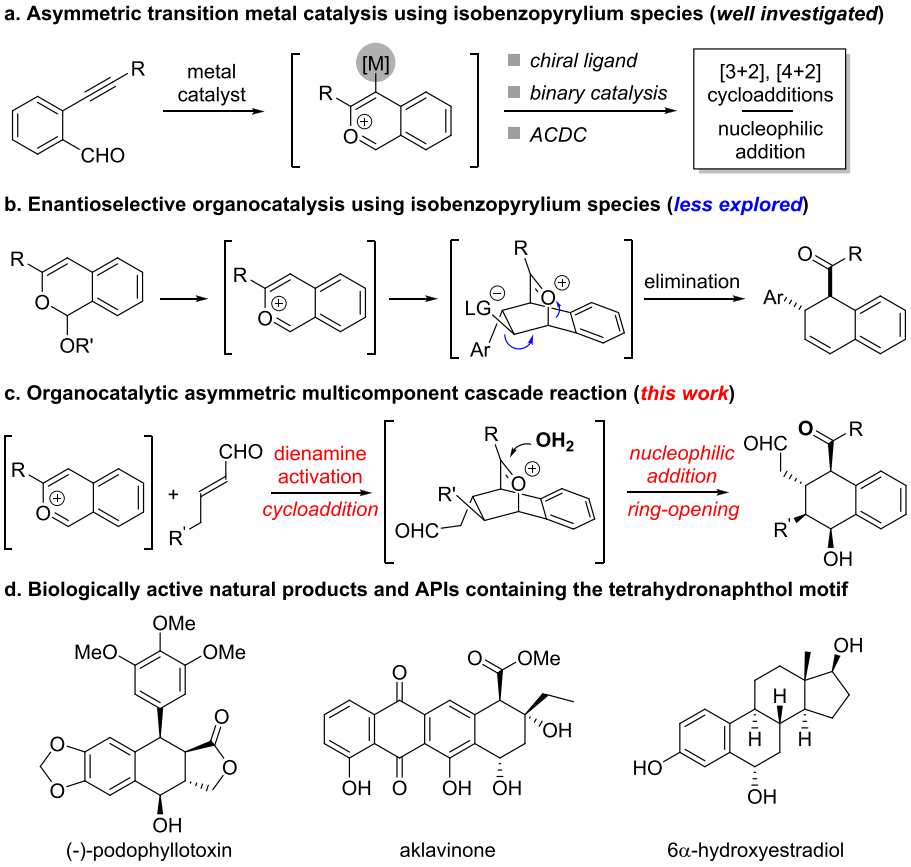

Figure 1. Generation and enantioselective reactions of isobenzopyrylium ions. (a) Activation by transition-metal complexes and reactions of the metallo-isobenzopyrylium intermediate. (b) Asymmetric synthesis of dihydronaphthalenes applying asymmetric counteranion-directed catalysis. (c) This work: organocatalytic formation of tetrahydronaphthols by enantioselective multicomponent cascade cycloaddition/nucleophilic addition/ring-opening reaction via dienamine catalysis. (d) Biologically active natural products and APIs containing the tetrahydronaphthol motif.

active pharmaceutical ingredients (API) and biologically active natural products (Figure 1d).[8] In addition, similar polycyclic ring systems can be accessed through simple transformations (*vide infra*).

Despite the intriguing scaffold of these molecules, the catalytic enantioselective construction of enantioenriched tetrahydronaphthols remains underdeveloped.[9] In previous studies, isobenzopyrylium ions displayed the ability to rapidly generate chiral dihydronaphthalenes by taking advantage of a cycloaddition reaction with alkenes as a key step.[10] The kinetic instability of the bridged oxonium intermediate, generated *in situ* from the initial cycloaddition reaction, led to an intramolecular elimination as the predominant pathway, consequently producing the carbon−carbon double bond present in the dihydronaphthalenes.

Alternatively, if the reactive oxocarbenium ion can be trapped by introduction of an appropriate nucleophile, such as H_2O,[11] tetrahydronaphthols might be accessed after ring-opening of the *in situ* generated cyclic hemiacetal. Dienamine catalysis can generate electron-rich olefins and has shown a high degree of stereocontrol in cycloadditions and good compatibility with water.[12] We envisioned that this presented an ideal strategy for a cascade sequence. Herein, we report the first asymmetric organocatalytic multicomponent cascade reaction involving isobenzopyrylium precursors, α,β-unsaturated aldehydes, and H_2O affording tetrahydronaphthols with four contiguous stereogenic centers with excellent selectivity. Furthermore, we present mechanistic investigations based on experimental and computational studies and finally cell painting experiments demonstrating the bioactivity of the scaffold.

■ RESULTS AND DISCUSSION

Optimization of Reaction Conditions. We initiated an investigation of the model reaction between 1-isopropoxy-3-phenyl-1*H*-isochromene (**1a**) and (*E*)-4-(4-methoxyphenyl)-but-2-enal (**2a**), in dichloromethane, at room temperature, in the presence of 20 mol % diphenyl phosphate (DPP), to examine the catalytic activities of various secondary amine catalysts **I**−**V**. The reactions catalyzed by **I**−**III** only delivered the dihydronaphthalene **3a′** in poor yield but excellent enantiomeric excess (Table 1, entries 1−3). When catalyst **IV** was employed in the reaction, the desired tetrahydronaphthol **3a** was obtained in low yield and moderate enantiomeric excess, together with **3a′** as a competing product (entry 4). No improvement in the yield of **3a**, or successful suppression of **3a′**, could be achieved from further screening of solvents (see the Supporting Information).

Considering that the elimination process affording dihydronaphthalene **3a′** may correlate with the Brønsted basicity of the aminocatalyst, the *gem*-difluorinated catalyst **V** was tested, and we were pleased that applying this catalyst afforded tetrahydronaphthol **3a** as the exclusive product in

https://doi.org/10.1021/jacs.1c03923
J. Am. Chem. Soc. 2021, 143, 8208−8220

Table 1. Optimization of the Reaction Conditions for the Organocatalytic Formation of Tetrahydronaphthols[a]

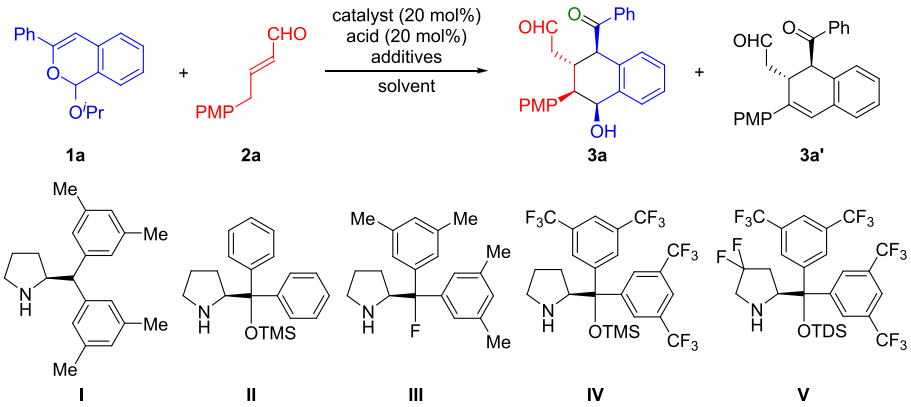

entry	cat.	acid[b]	additives (mol %)	solvent (0.1 M)[c]	T (°C)	yield (%)[d] 3a	yield (%)[d] 3a′	ee (%)[e] 3a	ee (%)[e] 3a′
1	**I**	DPP		CH_2Cl_2	rt		19		92
2	**II**	DPP		CH_2Cl_2	rt		29		96
3	**III**	DPP		CH_2Cl_2	rt		29		96
4	**IV**	DPP		CH_2Cl_2	rt	11	22	63	97
5	**V**	DPP		toluene	rt	41		78	
6	**V**	DPP		DME	rt	36		87	
7	**V**	DPP	$LiClO_4$ (100)	DME	rt	42		8	
8	**V**	DPP	$LiBF_4$ (100)	DME	rt	69		66	
9	**V**	DPP	LiOTf (100)	DME	rt	42		4	
10	**V**	DPP	H_2O (240)	DME	rt	45		92	
11	**V**	DPP	H_2O (240)/$LiBF_4$ (20)	DME	rt	83		88	
12	**V**	DPP	H_2O (240)/$LiBF_4$ (30)	DME	−20	92		94	
13[f]	**V**	HCl[g]	H_2O (240)/$LiBF_4$ (30)	DME	−20	89		96	

[a]Reactions were performed with **1a** (0.05 mmol), **2a** (0.075 mmol), catalyst (20 mol %), acid (20 mol %), and additives in solvent (0.5 mL) at specific temperature for 24 h. PMP = 4-methoxyphenyl. [b]DPP = diphenyl phosphate. [c]DME = 1,2-dimethoxyethane. [d]Yields were determined by ^{1}H NMR of the crude reaction mixture relative to an internal standard (tetraethylsilane). [e]Enantiomeric excess determined by chiral stationary phase UPCC after purification by FC. [f]Reaction performed on a 0.10 mmol scale. [g]HCl solution, 4 M in dioxane.

41% yield and 78% ee (entry 5). A survey of solvents revealed that 1,2-dimethoxyethane (DME) was the best choice (entry 6, see the Supporting Information). Additives were found to have an impact on the reactivity and stereoselectivity of the reaction (entries 7−9). Among them, $LiBF_4$ improved the yield significantly, but unfortunately with concurrent erosion of the enantioselectivity. The introduction of water (2.4 equiv) was shown to enhance the yield and enantiomeric excess (entry 10). Delightfully, product **3a** was obtained in 83% yield and 88% ee when water was present with a catalytic amount of $LiBF_4$ (entry 11). Subsequently, other reaction parameters, including the stoichiometry of additives and reaction temperature, were further evaluated to afford **3a** in 92% yield and 94% ee (entry 12 and the Supporting Information). Exchanging diphenyl phosphate for HCl led to the optimized reaction conditions (entry 13).

Scope of *α,β*-Unsaturated Aldehydes. With the optimized reaction conditions in hand, we then evaluated the substrate scope of this multicomponent cascade reaction for the stereoselective formation of tetrahydronaphthols. As shown in Table 2, *α,β*-unsaturated aldehydes **2** substituted with *γ*-aryl rings react with 1-isopropoxy-3-phenyl-1*H*-isochromene (**1a**) to afford the corresponding tetrahydronaphthols **3a−i** in high yields and excellent regio-, diastereo-, and enantioselectivities regardless of the electronic nature of the aromatic ring and the position of the substituent(s). The *α,β*-unsaturated aldehyde **2j** containing a benzo[*b*]thiophene group also provided product **3j** in high yield and enantioselectivity (93% ee). Crotonaldehyde proved to be compatible with the developed reaction, albeit product **3k** was obtained in only moderate yield (62%), but with excellent enantiomeric excess (93% ee). *α,β*-Unsaturated aldehydes with different alkyl groups, including methyl, propyl, and alkyl substituents bearing a 4-bromophenyl group, did not impact yield or enantioselectivity but did affect the diastereoselectivity (**3l−n**). Moreover, the reaction of **1a** with cyclopent-1-ene-1-carbaldehyde **2o** provided the tetrahydronaphthol product **3o** with an additional stereocenter, after increasing the temperature from −20 °C to room temperature. The absolute configuration of **3j** was determined by X-ray crystallographic analysis; the configurations of all other products were assigned by analogy and relevant 2D-NMR (see the Supporting Information).

Scope of Isochromenes. Next, we continued to investigate the substrate generality with respect to isochromenes **1** (Table 3). A variety of isochromenes with substituents on the 3-position were investigated. Electron-rich, -poor, and -neutral phenyl groups on the 3-position of the isochromenes uniformly gave excellent stereoselectivities and high yields (**4a−c**). The 2-naphthyl-substituted isochromene was also well tolerated, giving **4d**. Isochromenes carrying heteroaromatic substituents including furan and thiophene were successfully employed in the reaction

https://doi.org/10.1021/jacs.1c03923
J. Am. Chem. Soc. 2021, 143, 8208−8220

Table 2. Scope of α,β-Unsaturated Aldehydes for the Organocatalytic Enantioselective Formation of Tetrahydronaphthols[a]

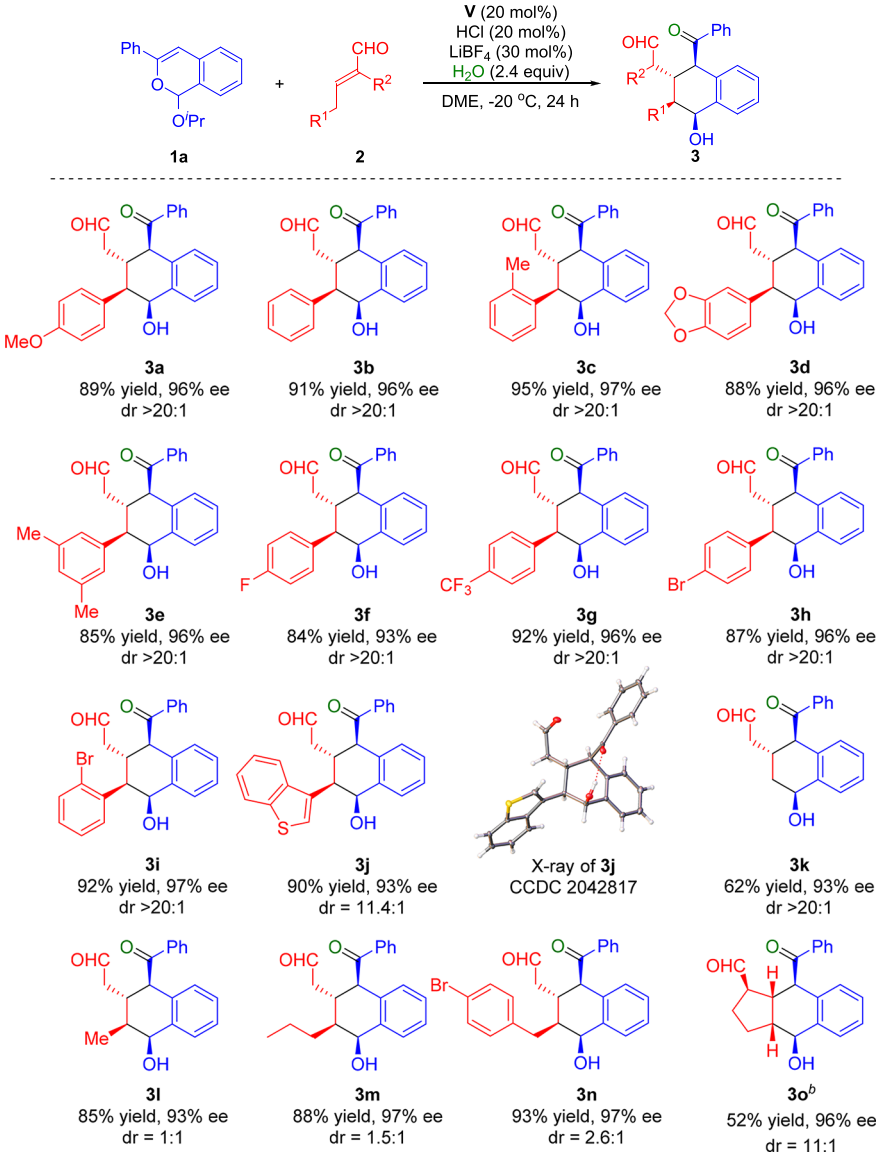

[a]Reactions were performed with **1a** (0.10 mmol), **2** (0.15 mmol), **V** (20 mol %), HCl (20 mol %, 4 M in dioxane), $LiBF_4$ (30 mol %), and H_2O (2.4 equiv) in DME (1.0 mL) at −20 °C for 24 h. In all cases, isolated yields are indicated. Enantiomeric excess determined by chiral stationary phase UPCC after purification by FC. The diastereomeric ratio was determined by ^{1}H NMR analysis. [b]Reaction was performed at rt.

sequence (**4e**,**f**). A TMS group could also be introduced, giving **4g** in relatively low yield but excellent stereoselectivity. Intriguingly, the isochromene with no substituents at the 3-position delivered hemiacetal **4h** as a stable compound, which could be isolated. Isochromenes having alkyl groups also reacted smoothly and showed high reactivity and selectivity regardless of being linear- or cycloalkyl-substituted (**4i**−**k**). Isochromene with a methoxy group at the 7-position or a fluoro group at the 6-position successfully formed the desired products **4l** or **4m**, respectively. Benzofused isochromene was also well tolerated, affording **4n** in high yield and excellent stereoselectivity. Interestingly, when employing benzothienopyrylium precursor **1p**, the eliminated compound **4o** was the only observed product. The exclusive formation of **4o** is probably due to the increased lability of the hydroxy group granted by the electron-rich ring-system, though this was not investigated further.

Oxygen-18-Labeling Studies.[13] To elucidate which oxygen atom is derived from the addition of H_2O in the tetrahydronaphthol adducts, ^{18}O-isotope-labeling experiments were performed with the intention of differentiating between the nucleophilic addition to the bridged oxonium intermediate by H_2O (Scheme 1, top, path a) or an S_N1 process after ring-opening of the intermediate (Scheme 1, top, path b).

The prototypical reaction between 1-isopropoxy-3-phenyl-1*H*-isochromene (**1a**) and (*E*)-4-(4-methoxyphenyl)but-2-enal (**2a**) was performed in the presence of 10 equiv of $H_2{}^{18}O$ (Scheme 1a), which was intended to dilute the concentration of advantageous H_2O (natural isotopic abundance) generated from the condensation of the α,β-unsaturated aldehyde **2a** and catalyst **V**. The ^{13}C NMR of the tetrahydronaphthol **3a** showed an efficient ^{18}O incorporation at the ketone[11c,d,f] of **3a** and no incorporation at the hydroxy group.

https://doi.org/10.1021/jacs.1c03923
J. Am. Chem. Soc. 2021, 143, 8208−8220

Table 3. Scope of Isochromenes for the Organocatalytic Enantioselective Formation of Tetrahydronaphthols[a]

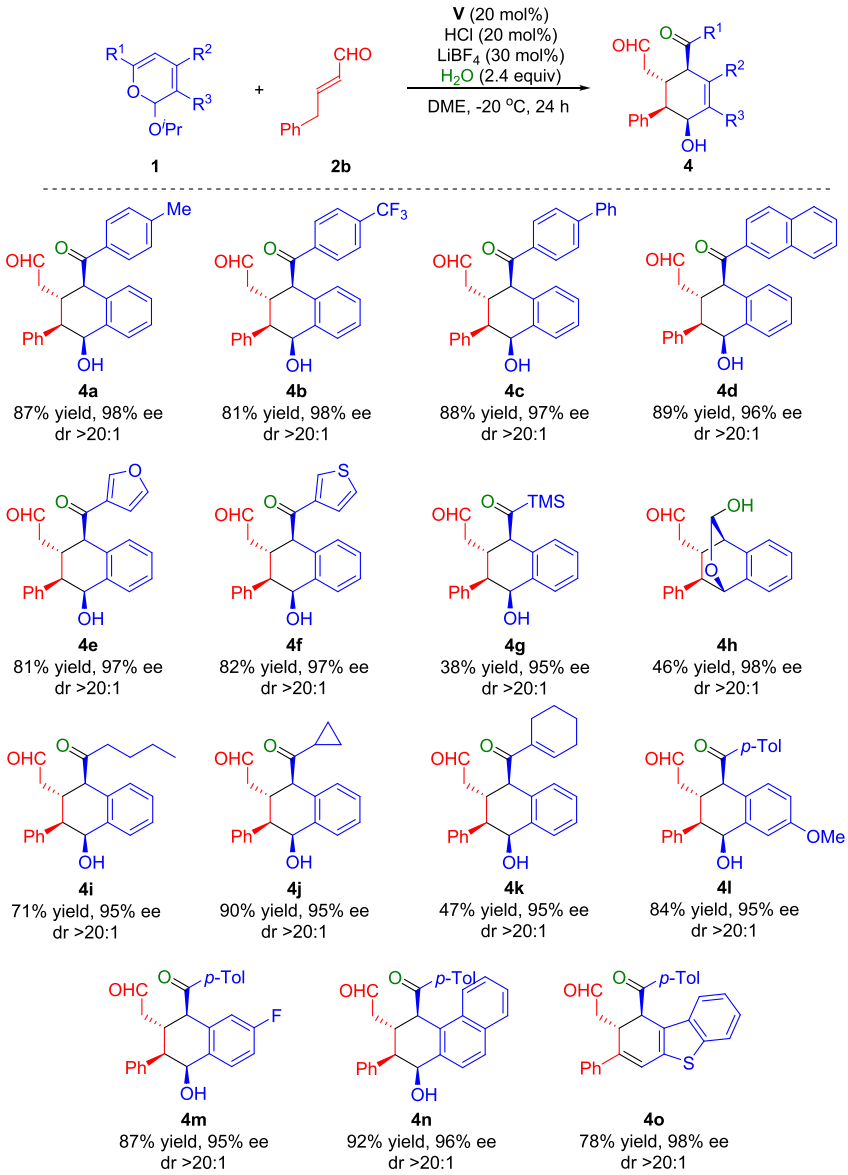

[a]Reactions were performed with **1** (0.10 mmol), **2b** (0.15 mmol), **V** (20 mol %), HCl (20 mol %, 4 M in dioxane), $LiBF_4$ (30 mol %), and H_2O (2.4 equiv) in DME (1.0 mL) at −20 °C for 24 h. In all cases, isolated yields are indicated. Enantiomeric excess determined by chiral stationary phase UPCC after purification by FC. The diastereomeric ratio was determined by ^{1}H NMR analysis.

To further confirm that the oxygen atom at the hydroxy group of the tetrahydronaphthol **3a** originates from 1-isopropoxy-3-phenyl-1*H*-isochromene (**1a**), ^{18}O-labeled **1a** bearing 28% ^{18}O at its isochromene ring was employed, resulting exclusively in ^{18}O incorporation at the hydroxy group of **3a** (Scheme 1b). These results support that the oxygen atom of the ketone in tetrahydronaphthol **3a** originates from external H_2O, and the oxygen atom of the benzylic alcohol originates from isochromene **1a**.

Catalytic Cycle and Computational Studies. With a basic understanding of the mechanism, we turned to modeling the reaction using density functional theory. Because of computational resource considerations, the theoretical investigation was performed on a model system. To ensure applicability of the calculations to the larger system, an experimental reaction was performed by using the model system (eq 1). Gratifyingly, the experiment was successful, and similar results to those observed with the full system were achieved.

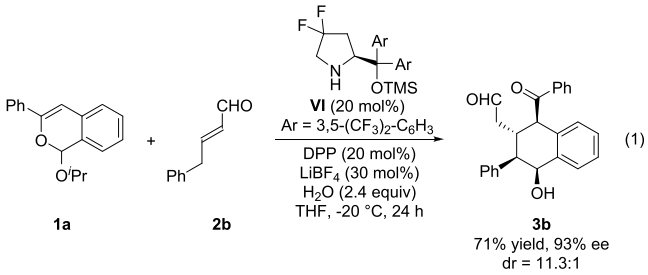

(1)

The model system was calculated by using the B3LYP functional with a 6-31G(d) basis set and SMD solvent continuum.[14] The single-point energies of the optimized structures were then calculated at the ωB97X-D/Def2-

https://doi.org/10.1021/jacs.1c03923
J. Am. Chem. Soc. 2021, 143, 8208−8220

Scheme 1. Oxygen-18-Labeling Studies to Trace the Origin of the Oxygen Atoms in the Tetrahydronaphthol Adduct: (a) the Reaction Was Performed in the Presence of $H_2{}^{18}O$ and (b) the Reaction Was Performed with ^{18}O-Labeled 1a

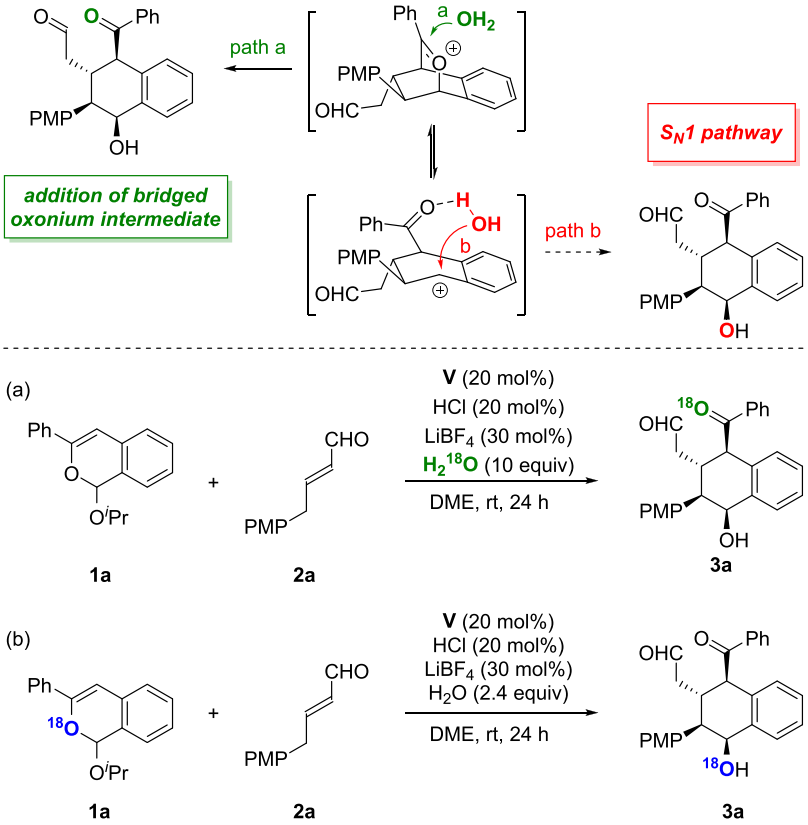

Scheme 2. Proposed Catalytic Cycle

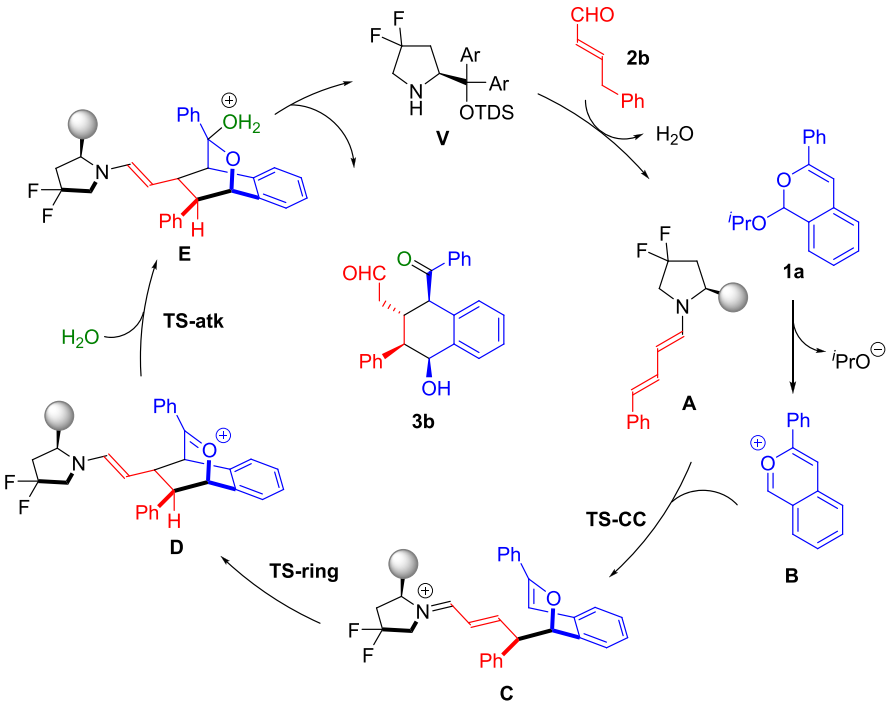

TZVPP/SMD level of theory.[15] All calculations were performed by using the Gaussian09 software package.[16] The free energies presented and discussed were calculated by applying the free energy correction from the lower level of theory optimization to the single point calculation.

The proposed catalytic cycle in Scheme 2 begins with the condensation of (*E*)-4-phenylbut-2-enal (**2b**) with the catalyst **V** to form dienamine intermediate **A**. After the isobenzopyrylium ion intermediate **B** is generated by expulsion of the isopropoxide leaving group from 1-isopropoxy-3-phenyl-1*H*-

https://doi.org/10.1021/jacs.1c03923
J. Am. Chem. Soc. 2021, 143, 8208−8220

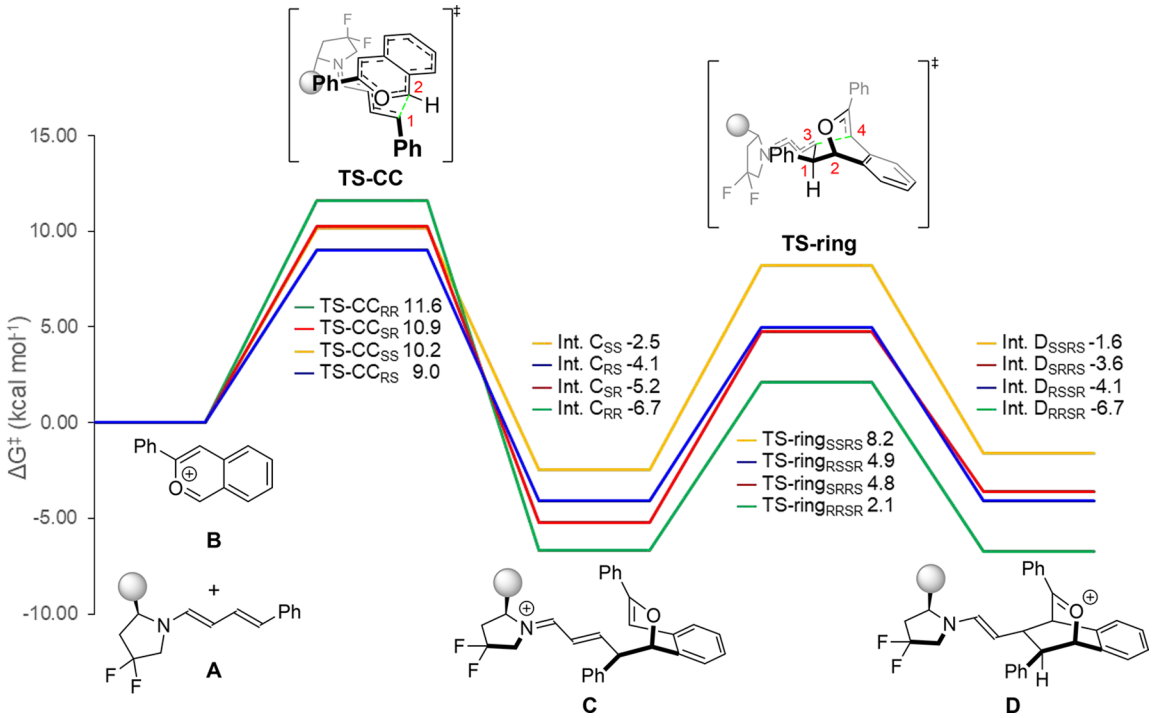

Figure 2. Free energy profile for the multicomponent cascade reaction between **1a** and **2b**; **TS-CC** for all possible diastereomeric outcomes and the lowest four **TS-ring** energies leading to the theoretically preferred diastereomers; ωB97XD/Def2-TZVPP/SMD(THF)//B3LYP/6-31G(d)/SMD(THF).

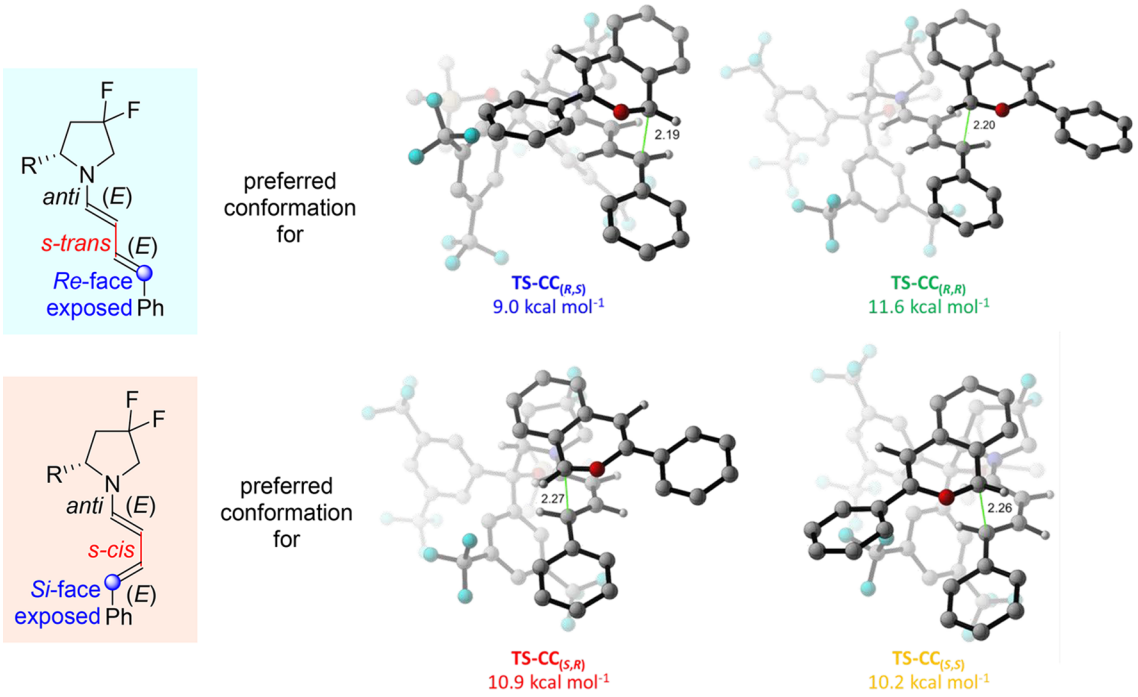

Figure 3. Geometries for optimized **TS-CC** for all possible stereochemical outcomes. Calculations performed by using ωB97X-D/Def2-TZVPP/SMD//B3LYP/6-31G(d)/SMD; some atoms are not shown for clarity (distances in angstroms).

isochromene (**1a**), intermediate **B** is attacked by the γ-position of dienamine **A** forming the initial carbon−carbon bond via **TS-CC** to afford intermediate **C**. Ring-closure, via **TS-ring**, then generates intermediate **D**. Addition of water at the carbonyl carbon generates intermediate **E**. A series of proton transfers, final C−O bond scission, and hydrolysis yield product **3b** and afford catalyst turnover.

Computational and NMR investigations into the nature of dienamines have shown that the species tend to exist as a mixture of isomers with rapidly converting double bonds from protonation/deprotonation events and a mixture of *s-cis* and *s-trans* conformers from rotating σ-bonds.[17]

A systematic search of transition-state structures corresponding to **TS-CC** and **TS-ring** was performed exploring all

https://doi.org/10.1021/jacs.1c03923
J. Am. Chem. Soc. 2021, 143, 8208−8220

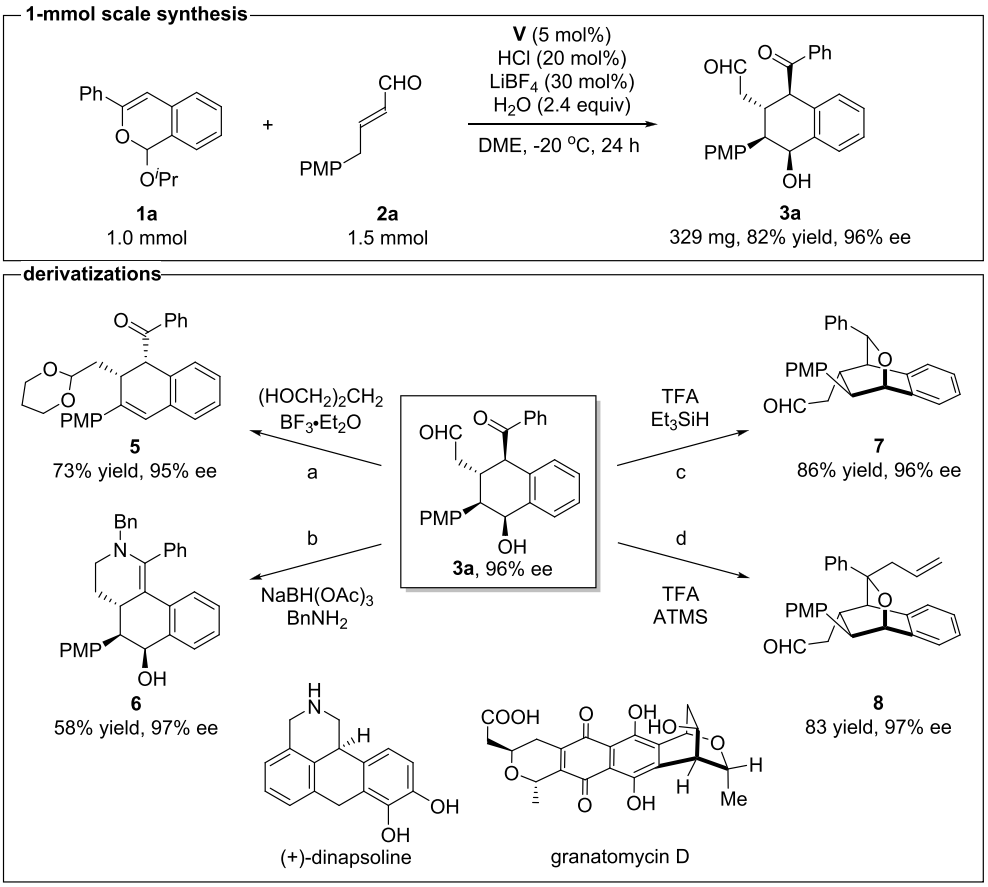

Figure 4. Examples of transformations and relations to an API and a natural product. (a) Selective protection and elimination of **3a**. (b) Reductive amination of product **3a**. (c) Reductive etherification of **3a** to afford a bicyclo[2.2.2]octane framework. (d) Reductive allylation protocol to afford bicyclo-ether **8**.

possible stereoisomers and conformations (see the Supporting Information). After obtaining a basic understanding of the potential energy surface, it became clear that **TS-CC** was responsible for both the observed enantioselectivity as well as the diastereoselectivity. The predicted barrier for the transition state leading to the observed product is 9.0 kcal mol^{-1} (Figure 2). The pathway leading to the enantiomer of this product is 1.9 kcal mol^{-1} higher (10.9 kcal mol^{-1}), leading to a predicted enantiomeric excess of 96% ee, which is in good agreement with experimental data (eq 1). The lowest diastereomer is calculated to have a $\Delta G^{\ddagger}$ of 10.2 kcal mol^{-1}. This leads to a predicted diastereomeric ratio of 11:1, which again is in good agreement with the observed selectivity (eq 1).

With the selectivity correctly predicted by our calculations, we found it interesting to observe how dienamine **A** orients itself in the reaction. It has been the argument with this type of catalyst the incoming reacting partner prefers to approach from the *opposite* face of the steric bulk of the catalyst.[18] The least sterically demanding conformation of **A** is to have the C−N bond connecting the catalyst to the carbon−carbon chain of the dienamine in an *anti*-conformation, the σ-bond between the two π-systems of the dienamine in an *s-trans*-conformation, and both double bonds in an *E*-conformation. The *E*/*Z* nature of these systems has been well explored with *E*-conformers being preferred.[17]

For **TS-CC**$_{(R,S)}$ and **TS-CC**$_{(R,R)}$, aligning the σ-bonds in this *anti*- and *s-trans*-conformation was simple as the *Re*-face is pointed away from the bulk of the catalyst (Figure 3, top). In the case of **TS-CC**$_{(S,R)}$ and **TS-CC**$_{(S,S)}$, with the *Si*-face forming the initial carbon−carbon bond, one of the σ-bonds was required to rotate. It was found that rotating the C−C bond between the π-systems granted the lowest energy transition-state structure, meaning that these products prefer the *s-cis* conformation to minimize steric interaction with the catalyst (Figure 3, bottom). As a consequence of this conformation, the energies of these transition states increase, thus leading to the observed stereoselectivity.

The observed selectivity between **TS-CC**$_{(R,S)}$ and **TS-CC**$_{(R,R)}$ can be explained by the fact that the appended phenyl ring of the isobenzopyrylium ion must be pointed away from the catalyst to minimize steric interaction. As such, in **TS-CC**$_{(R,R)}$, the π-system of **A** is not overlapping with that of **B**. The lack of this interaction is proposed to be the major contributor to the higher predicted energy as supported by noncovalent interaction (NCI) analysis (see the Supporting Information).

Computational investigation next turned to the nature of the cycloaddition at hand. Previously, similar reactions have been termed [4 + 2] cycloadditions,[5c,g,6a,b] but recent investigation in our group has suggested that a system will prefer to react with the most π-electrons available.[19] For a discussion of the possible number of π-electrons involved in the cycloaddition, see the Supporting Information.

Transformations. To demonstrate the synthetic utility of the multicomponent cascade reaction, a 1 mmol scale

https://doi.org/10.1021/jacs.1c03923
J. Am. Chem. Soc. 2021, 143, 8208−8220

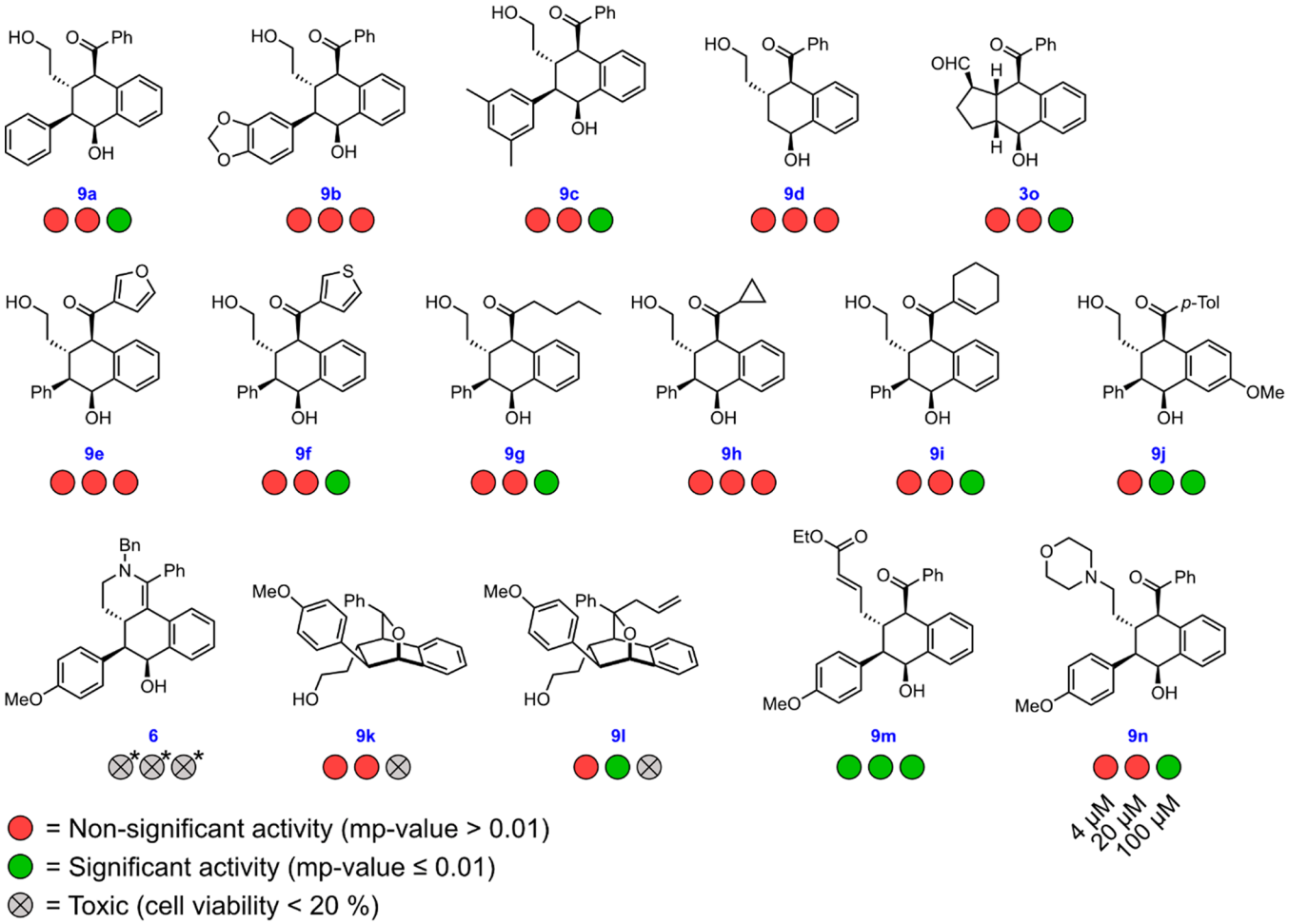

Figure 5. Structures of compounds tested in the cell painting assay. The colored circles indicate the activity in the cell painting assay; see Figure 6 and the Supporting Information for details. *Compound **6** precipitated at the tested concentrations, causing unspecific cell death to a varying degree.

synthesis of 1-isopropoxy-3-phenyl-1*H*-isochromene (**1a**) and (*E*)-4-(4-methoxyphenyl)but-2-enal (**2a**) was performed with a catalyst loading of 5 mol %. To our delight, the reaction proceeded smoothly to give product **3a** in 82% yield, without erosion of enantioselectivity (96% ee, Figure 4, top). The tetrahydronaphthol **3a** obtained herein can be readily converted into synthetically useful compounds in a facile manner. The aldehyde functionality in **3a** was selectively protected by treatment with 1,3-propanediol and $BF_3{\cdot}Et_2O$. Concomitant elimination of the benzylic hydroxy group took place as well as epimerization of the stereocenter at the α-carbon of the carbonyl in **5** (Figure 4a). The sequential reductive amination of **3a** produced compound **6** in 58% yield and maintained enantioselectivity (Figure 4b). The octahydrobenzo[*h*]isoquinoline scaffold of **6** is the core structure of many dopamine agonists like dinapsoline, an API developed for the treatment of Parkinson's disease.[20] Treatment of **3a** with TFA and nucleophilic reagents, such as triethylsilane and allyltrimethylsilane (ATMS), resulted in the formation of **7** and **8** bearing [2.2.2]octane frameworks which are widely present in biologically active natural products[21] (Figure 4c,d).

Bioactivity. As the tetrahydronaphthol scaffold is present in various biologically active compounds, we set out to investigate whether the compounds possessed bioactivity. To facilitate the testing of bioactivity, we derivatized a number of compounds providing **9a**−**9n** (Figure 5; see the Supporting Information), which, together with compounds **6** and **3o**, were submitted to the cell painting assay (Figure 6).[22]

Cell painting (Figure 6a) monitors the morphological changes induced by compound treatment by fluorescence microscopy. By performing quantitative image analysis, a large number of morphological features can be extracted, yielding a profile representing the bioactivity of the treatment (Figure 6a). The profile contains various information: From the strength of a profile a bioactivity score (Mahalanobis distance) can be calculated, and it can be determined if the change is statistically significantly different from DMSO treatment (mp value ≤0.01).[23] Furthermore, the profile encodes the mechanism, as a morphological fingerprint, by which the compound induces morphological changes and can thus be used to determine if compounds have similar or different bioactivity. We tested the 16 compounds at 100, 20, and 4 μM in U-2OS osteosarcoma cells. Of the 16 compounds, 63% (10 out of 16) induced significant morphological changes, indicating that the scaffold is enriched for biological activity (see Figure S9). Compounds **9k** and **9l** were toxic at 100 μM, reducing the cell viability to <20%, while compound **6** was insoluble at the test concentrations. The morphological profiles (Figure 6c) of

https://doi.org/10.1021/jacs.1c03923
J. Am. Chem. Soc. 2021, 143, 8208−8220

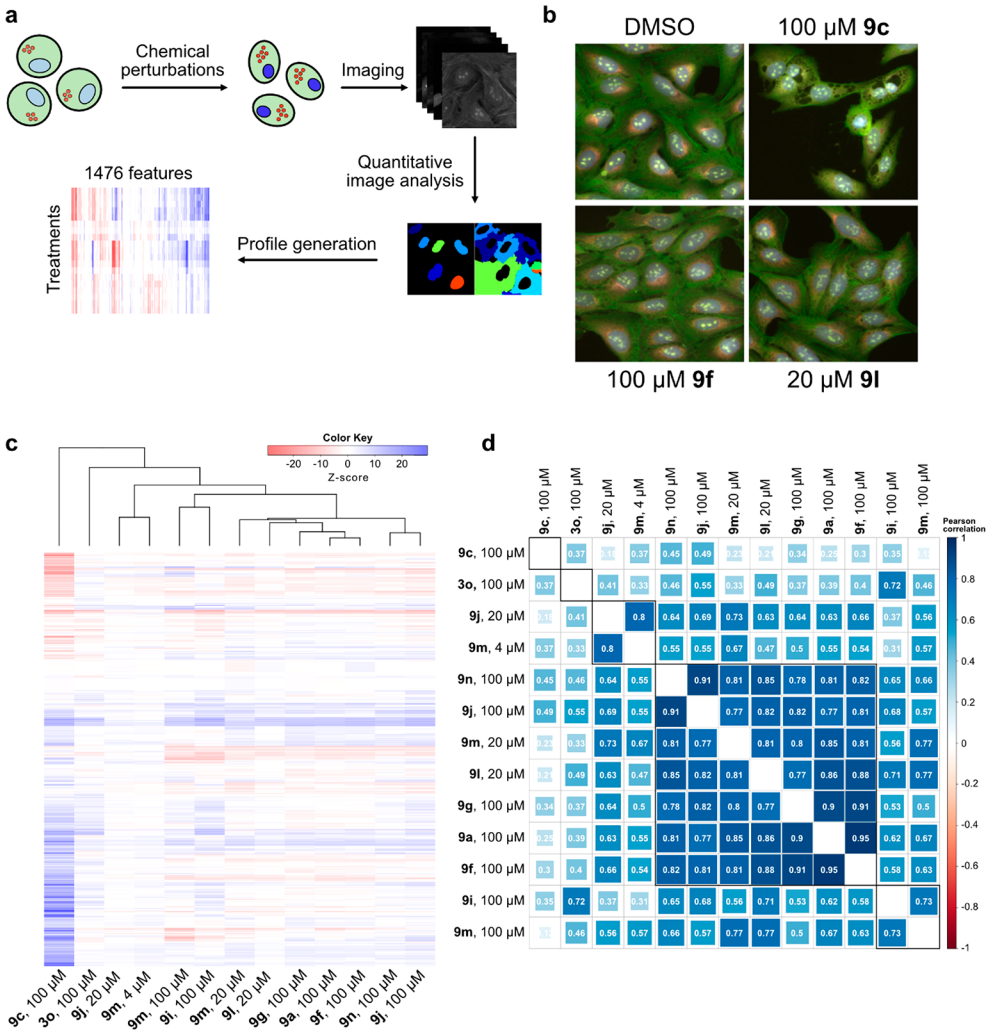

Figure 6. Bioactivity determination by morphological profiling. (a) Principle of morphological profiling via the cell painting assay. (b) Merge of fluorescence microscopy images from the cell painting assay (see Figure S10 for individual channels). (c) Heatmap of morphological profiles from nontoxic and significant active treatments. (d) Correlation matrix of nontoxic and significantly active profiles.

the active and nontoxic compounds were compared by calculating the Pearson correlation coefficient and clustering the compounds based on hierarchical clustering (Figure 6d). Most compounds induced similar morphological changes indicated by a large cluster with high cross-correlations (0.77−0.95), which is unsurprising considering the structural similarities between these compounds. The compounds in this cluster induced subtle morphological changes, not readily obvious by visible inspection (Figure 6b). Intriguingly, some compounds such as **3o** (100 μM) and **9c** (100 μM) induced a more unique profile, with compound **9c** causing a clear morphological change (Figure 6b), distinct from any other compounds in this small collection. The mechanism of action behind these compounds is subject to further investigations.

■ CONCLUSION

In summary, we performed an organocatalytic asymmetric multicomponent cascade reaction employing isobenzopyrylium precursors, α,β-unsaturated aldehydes, and water via dienamine catalysis. Tetrahydronaphthols with up to five contiguous stereocenters were prepared in high yield with excellent diastereo- and enantioselectivity. The substrate scope is broad, and the tetrahydronaphthols can be readily converted into synthetically useful compounds demonstrating the power and importance of the development of a new synthetic method utilizing isobenzopyrylium ions. ^{18}O-isotope-labeling experiments and theoretical studies provided evidence for the reaction process and stereochemistry. We finally show that a collection of tetrahydronaphthol compounds possesses bioactivity in U-2OS cancer cells by monitoring morphological changes.

■ ASSOCIATED CONTENT

Supporting Information

The Supporting Information is available free of charge at https://pubs.acs.org/doi/10.1021/jacs.1c03923.

Experimental procedures, characterization data, NMR spectra, UPCC spectra, and theoretical calculations (PDF)

Accession Codes

CCDC 2042817 contains the supplementary crystallographic data for this paper. These data can be obtained free of charge via www.ccdc.cam.ac.uk/data_request/cif, or by emailing data_request@ccdc.cam.ac.uk, or by contacting The Cam-

https://doi.org/10.1021/jacs.1c03923
J. Am. Chem. Soc. 2021, 143, 8208−8220

bridge Crystallographic Data Centre, 12 Union Road, Cambridge CB2 1EZ, UK; fax: +44 1223 336033.

■ AUTHOR INFORMATION

Corresponding Author

Karl Anker Jørgensen − *Department of Chemistry, Aarhus University, DK-8000 Aarhus C, Denmark;* orcid.org/0000-0002-3482-6236; Email: kaj@chem.au.dk

Authors

Yidong Liu − *Department of Chemistry, Aarhus University, DK-8000 Aarhus C, Denmark;* orcid.org/0000-0002-7988-8908

Joseph A. Izzo − *Department of Chemistry, Aarhus University, DK-8000 Aarhus C, Denmark;* orcid.org/0000-0002-2875-2138

David McLeod − *Department of Chemistry, Aarhus University, DK-8000 Aarhus C, Denmark*

Sebastijan Ričko − *Department of Chemistry, Aarhus University, DK-8000 Aarhus C, Denmark*

Esben B. Svenningsen − *Department of Chemistry, Aarhus University, DK-8000 Aarhus C, Denmark;* orcid.org/0000-0001-5118-6499

Thomas B. Poulsen − *Department of Chemistry, Aarhus University, DK-8000 Aarhus C, Denmark;* orcid.org/0000-0002-0763-9996

Complete contact information is available at: https://pubs.acs.org/10.1021/jacs.1c03923

Notes

The authors declare no competing financial interest.

■ ACKNOWLEDGMENTS

K.A.J. thanks Villum Investigator Grant 25867, the Carlsberg Foundation "Semper Ardens", and Aarhus University. The computational results presented in this work were obtained at the Centre for Scientific Computing, Aarhus (http://phys.au.dk/forskning/cscaa/). Thanks are expressed to Mathias Kirk Thøgersen for performing the crystallographic work. S.R. was supported by the European Union Horizon 2020 Research and Innovation Programme under the Marie Skłodowska-Curie Grant Agreement 754513 and by Aarhus University Research Foundation (AIAS-COFUND). Financial support from the Slovenian Research Agency through Grant P1-0179 is also gratefully acknowledged. T.B.P. acknowledges the Carlsberg Foundation (Grant CF17-0800) for financial support.

■ REFERENCES

(1) (a) Tietze, L. F.; Brasche, G.; Gericke, K. M. *Domino Reactions in Organic Synthesis*; Wiley-VCH: Weinheim, Germany, 2006; pp 1−631. (b) Xu, P. F.; Wang, W. *Catalytic Cascade Reactions*; Wiley-VCH: Weinheim, Germany, 2014; pp 1−440. (c) Wang, Q.; Zhu, J. *Multicomponent Domino Process: Rational Design and Serendipity*; Wiley-VCH: Weinheim, Germany, 2014; pp 579−610.

(2) For selected reviews, see: (a) Grossmann, A.; Enders, D. N-Heterocyclic Carbene Catalyzed Domino Reactions. *Angew. Chem., Int. Ed.* **2012**, *51*, 314−325. (b) Alemán, J.; Cabrera, S. Applications of Asymmetric Organocatalysis in Medicinal Chemistry. *Chem. Soc. Rev.* **2013**, *42*, 774−793. (c) Denard, C. A.; Hartwig, J. F.; Zhao, H. Multistep One-Pot Reactions Combining Biocatalysts and Chemical Catalysts for Asymmetric Synthesis. *ACS Catal.* **2013**, *3*, 2856−2864. (d) Volla, C. M. R.; Atodiresei, I.; Rueping, M. Catalytic C-C Bond-Forming Multi-Component Cascade or Domino Reactions: Pushing the Boundaries of Complexity in Asymmetric Organocatalysis. *Chem. Rev.* **2014**, *114*, 2390−2431. (e) Walsh, C. T.; Moore, B. S. Enzymatic Cascade Reactions in Biosynthesis. *Angew. Chem., Int. Ed.* **2019**, *58*, 6846−6879. (f) Pellissier, H. Recent Developments in Enantioselective Multicatalyzed Tandem Reactions. *Adv. Synth. Catal.* **2020**, *362*, 2289−2325.

(3) For selected reviews, see: (a) Santamaría, J.; Valdés, C. Six-Membered Rings with One Oxygen: Pyrylium Ion, Related Systems and Benzo-Derivatives. In *Modern Heterocyclic Chemistry*; Alvarez-Builla, J., Vaquero, J. J., Barluenga, J., Eds.; Wiley-VCH: Weinheim, Germany, 2011; Vol. 3, pp 1631−1682. (b) Kuznetsov, E. V.; Shcherbakova, I. V.; Balaban, A. T. Benzo[*c*]Pyrylium Salts: Syntheses, Reactions, and Physical Properties. *Adv. Heterocycl. Chem.* **1990**, *50*, 157−254. (c) Hein, S. J.; Lehnherr, D.; Arslan, H.; Uribe-Romo, F. J.; Dichtel, W. R. Alkyne Benzannulation Reactions for the Synthesis of Novel Aromatic Architectures. *Acc. Chem. Res.* **2017**, *50*, 2776−2788. (d) Chen, L.; Chen, K.; Zhu, S. Transition-Metal-Catalyzed Intramolecular Nucleophilic Addition of Carbonyl Groups to Alkynes. *Chem.* **2018**, *4*, 1208−1262. (e) Chen, L.; Liu, Z.; Zhu, S. Donor- and Acceptor-Enynals/enynones. *Org. Biomol. Chem.* **2018**, *16*, 8884−8898.

(4) Chen, J. R.; Hu, X.-Q.; Xiao, W.-J. Metal-Containing Carbonyl Ylides: Versatile Reactants in Catalytic Enantioselective Cascade Reactions. *Angew. Chem., Int. Ed.* **2014**, *53*, 4038−4040.

(5) (a) Suga, H.; Inoue, K.; Inoue, S.; Kakehi, A. Highly Enantioselective 1,3-Dipolar Cycloaddition Reactions of 2-Benzopyrylium-4-olate Catalyzed by Chiral Lewis Acids. *J. Am. Chem. Soc.* **2002**, *124*, 14836−14837. (b) Suga, H.; Inoue, K.; Inoue, S.; Kakehi, A.; Shiro, M. Chiral 2,6-Bis(oxazolinyl)pyridine-Rare Earth Metal Complexes as Catalysts for Highly Enantioselective 1,3-Dipolar Cycloaddition Reactions of 2-Benzopyrylium-4-olates. *J. Org. Chem.* **2005**, *70*, 47−56. (c) Hojo, D.; Noguchi, K.; Tanaka, K. Synthesis of Chiral Tetrasubstituted Alkenes by an Asymmetric Cascade Reaction Catalyzed Cooperatively by Cationic Rhodium(I) and Silver(I) Complexes. *Angew. Chem., Int. Ed.* **2009**, *48*, 8129−8132. (d) Handa, S.; Slaughter, L. M. Enantioselective Alkynylbenzaldehyde Cyclizations Catalyzed by Chiral Gold(I) Acyclic Diaminocarbene Complexes Containing Weak Au-Arene Interactions. *Angew. Chem., Int. Ed.* **2012**, *51*, 2912−2915. (e) Terada, M.; Toda, Y. Relay Catalysis Using a Rhodium Complex/Chiral Brønsted Acid Binary System: Enantioselective Reduction of a Carbonyl Ylide as the Reactive Intermediate. *Angew. Chem., Int. Ed.* **2012**, *51*, 2093−2097. (f) Saito, K.; Kajiwara, Y.; Akiyama, T. Chiral Copper(II) Phosphate Catalyzed Enantioselective Synthesis of Isochromene Derivatives by Sequential Intramolecular Cyclization and Asymmetric Transfer Hydrogenation of *o*-Alkynylacetophenones. *Angew. Chem., Int. Ed.* **2013**, *52*, 13284−13288. (g) Yu, S.-Y.; Zhang, H.; Gao, Y.; Mo, L.; Wang, S.; Yao, Z.-J. Asymmetric Cascade Annulation Based on Enantioselective Oxa-Diels-Alder Cycloaddition of in Situ Generated Isochromenyliums by Cooperative Binary Catalysis of $Pd(OAc)_2$ and (*S*)-Trip. *J. Am. Chem. Soc.* **2013**, *135*, 11402−11407. (h) Terada, M.; Li, F.; Toda, Y. Chiral Silver Phosphate Catalyzed Transformation of *ortho*-Alkynylaryl Ketones into 1*H*-Isochromene Derivatives through an Intramolecular-Cyclization/Enantioselective-Reduction Sequence. *Angew. Chem., Int. Ed.* **2014**, *53*, 235−239. (i) Miao, T.; Tian, Z.-Y.; He, Y.-M.; Chen, F.; Chen, Y.; Yu, Z.-X.; Fan, Q.-H. Asymmetric Hydrogenation of In Situ Generated Isochromenylium Intermediates by Copper/Ruthenium Tandem Catalysis. *Angew. Chem., Int. Ed.* **2017**, *56*, 4135−4139. (j) Bröhl, N. F.; Kundu, D. S.; Raabe, G.; Enders, D. One-Pot Synthesis of 1-Substituted 1*H*-Isochromenes by Combining Brønsted Acid with Silver Catalysis. *Synthesis* **2017**, *49*, 1243−1254. (k) Cai, L.; Chen, Y.; Cao, H.; Wei, Q.; Yang, Y.; Ouyang, Q.; Peng, Y. Asymmetric Cyclization/Nucleophilic Tandem Reaction of *o*-Alkynylacetophenone with (Diazomethyl)phosphonate for the Synthesis of Functional Isochromenes. *Org. Lett.* **2019**, *21*, 7597−7601.

(6) (a) Qian, H.; Zhao, W.; Wang, Z.; Sun, J. Organocatalytic Enantio- and Diastereoselective Synthesis of 1,2-Dihydronaphtha-

lenes from Isobenzopyrylium Ions. *J. Am. Chem. Soc.* **2015**, *137*, 560−563. (b) Luan, Y.; Barbato, K. S.; Moquist, P. N.; Kodama, T.; Schaus, S. E. Enantioselective Synthesis of 1,2-Dihydronaphthalene-1-carbaldehydes by Addition of Boronates to Isochromene Acetals Catalyzed by Tartaric Acid. *J. Am. Chem. Soc.* **2015**, *137*, 3233−3236. (c) Wan, M.; Sun, S.; Li, Y.; Liu, L. Organocatalytic Redox Deracemization of Cyclic Benzylic Ethers Enabled by An Acetal Pool Strategy. *Angew. Chem., Int. Ed.* **2017**, *56*, 5116−5120.

(7) (a) Wang, Y.-B.; Tan, B. Construction of Axially Chiral Compounds via Asymmetric Organocatalysis. *Acc. Chem. Res.* **2018**, *51*, 534−547. (b) Metrano, A. J.; Miller, S. J. Peptide-Based Catalysts Reach the Outer Sphere through Remote Desymmetrization and Atroposelectivity. *Acc. Chem. Res.* **2019**, *52*, 199−215. (c) Sheng, F.-T.; Wang, J.-Y.; Tan, W.; Zhang, Y.-C.; Shi, F. Progresses in Organocatalytic Asymmetric Dearomatization Reactions of Indole Derivatives. *Org. Chem. Front.* **2020**, *7*, 3967−3998. (d) Zhang, Y.-C.; Jiang, F.; Shi, F. Organocatalytic Asymmetric Synthesis of Indole-Based Chiral Heterocycles: Strategies, Reactions, and Outreach. *Acc. Chem. Res.* **2020**, *53*, 425−446.

(8) (a) Ayres, D. C.; Loike, J. D. *Lignans: Chemical, Biological and Clinical Properties*; Cambridge University Press: Cambridge, UK, 1990; pp 1−402. (b) Imbert, T. F. Discovery of Podophyllotoxins. *Biochimie* **1998**, *80*, 207−222. (c) Ward, R. S. Lignans, Neolignans and Related Compounds. *Nat. Prod. Rep.* **1999**, *16*, 75−96. (d) Wander, D. P. A.; van der Zanden, S. Y.; van der Marel, G. A.; Overkleeft, H. S.; Neefjes, J.; Codée, J. D. C. Doxorubicin and Aclarubicin: Shuffling Anthracycline Glycans for Improved Anticancer Agents. *J. Med. Chem.* **2020**, *63*, 12814−12829.

(9) (a) Quinkert, G.; Stark, H. Stereoselective Synthesis of Enantiomerically Pure Natural Products-Estrone as Example. *Angew. Chem., Int. Ed. Engl.* **1983**, *22*, 637−655. (b) Kraus, G. A.; Wu, Y. Hydrogen Atom Abstraction Reactions in Organic Synthesis. A Formal Total Synthesis of Racemic Podophyllotoxin. *J. Org. Chem.* **1992**, *57*, 2922−2925. (c) Nicolaou, K. C.; Gray, D. Total Synthesis of Hybocarpone. *Angew. Chem., Int. Ed.* **2001**, *40*, 761−763. (d) Grosch, B.; Orlebar, C. N.; Herdtweck, E.; Massa, W.; Bach, T. Highly Enantioselective Diels-Alder Reaction of a Photochemically Generated *o*-Quinodimethane with Olefins. *Angew. Chem., Int. Ed.* **2003**, *42*, 3693−3696. (e) Nicolaou, K. C.; Gray, D. L. F.; Tae, J. Total Synthesis of Hamigerans and Analogues Thereof. Photochemical Generation and Diels-Alder Trapping of Hydroxy-*o*-Quinodimethanes. *J. Am. Chem. Soc.* **2004**, *126*, 613−627. (f) Capriati, V.; Florio, S.; Luisi, R.; Perna, F. M.; Salomone, A.; Gasparrini, F. An Efficient Route to Tetrahydronaphthols *via* Addition of *ortho*-Lithiated Stilbene Oxides to α,β-Unsaturated Fischer Carbene Complexes. *Org. Lett.* **2005**, *7*, 4895−4898. (g) Zhu, S.; Liang, R.; Jiang, H.; Wu, W. An Efficient Route to Polysubstituted Tetrahydronaphthols: Silver-Catalyzed [4 + 2] Cyclization of 2-Alkylbenzaldehydes and Alkenes. *Angew. Chem., Int. Ed.* **2012**, *51* (7), 10861−10865. (h) Dell'Amico, L.; Vega-Peñaloza, A.; Cuadros, S.; Melchiorre, P. Enantioselective Organocatalytic Diels-Alder Trapping of Photochemically Generated Hydroxy-*o*-Quinodimethanes. *Angew. Chem., Int. Ed.* **2016**, *55*, 3313−3317. (i) Li, H.; Wang, Y.; Lai, Z.; Huang, K.-W. Selective Catalytic Hydrogenation of Arenols by a Well-Defined Complex of Ruthenium and Phosphorus-Nitrogen PN^3-Pincer Ligand Containing a Phenanthroline Backbone. *ACS Catal.* **2017**, *7*, 4446−4450.

(10) (a) Asao, N.; Kasahara, T.; Yamamoto, Y. Functionalized 1,2-Dihydronaphthalenes from the $Cu(OTf)_2$-Catalyzed [4 + 2] Cycloaddition of *o*-Alkynyl(oxo)benzenes with Alkenes. *Angew. Chem., Int. Ed.* **2003**, *42*, 3504−3506. (b) Hu, Z.-L.; Qian, W.-J.; Wang, S.; Wang, S.; Yao, Z.-J. Transformation of Reactive Isochromenylium Intermediates to Stable Salts and Their Cascade Reactions with Olefins. *Org. Lett.* **2009**, *11*, 4676−4679. (c) Malhotra, D.; Liu, L.-P.; Mashuta, M. S.; Hammond, G. B. Gold-Catalyzed Annulations of 2-Alkynyl Benzaldehydes with Vinyl Ethers: Synthesis of Dihydronaphthalene, Isochromene, and Bicyclo[2.2.2]octane Derivatives. *Chem. - Eur. J.* **2013**, *19*, 4043−4050. (d) Ruch, A. A.; Kong, F.; Nesterov, V. N.; Slaughter, L. M. Tetracyclic Dihydronaphthalene Derivatives *via* Gold-Catalyzed Aminative Homodimerization of *ortho*-Alkynylbenzaldehydes. *Chem. Commun.* **2016**, *52*, 14133−14136. (e) Zhang, C.; Chen, L.; Chen, K.; Jiang, H.; Zhu, S. Iron/Zinc-Catalyzed Benzannulation Reactions of 2-(2-oxo-Alkyl)benzketones Leading to Naphthalene and Isoquinoline Derivatives. *Org. Chem. Front.* **2018**, *5*, 1028−1033.

(11) (a) Dyker, G.; Hildebrandt, D.; Liu, J.; Merz, K. Gold(III) Chloride Catalyzed Domino Processes with Isobenzopyrylium Cation Intermediates. *Angew. Chem., Int. Ed.* **2003**, *42*, 4399−4402. (b) Beeler, A. B.; Su, S.; Singleton, C. A.; Porco, J. A., Jr. Discovery of Chemical Reactions through Multidimensional Screening. *J. Am. Chem. Soc.* **2007**, *129*, 1413−1419. (c) Luo, H.; Liang, R.; Chen, L.; Jiang, H.; Zhu, S. A Silver-Catalyzed Three-Component Reaction *via* Stabilized Cation: Synthesis of Polysubstituted Tetrahydronaphthols and Tetrahydronaphthylamines. *Org. Chem. Front.* **2018**, *5*, 1160−1164. (d) Giri, S. S.; Liu, R.-S. Copper-Catalyzed [4 + 2]-Cycloadditions of Isoxazoles with 2-Alkynylbenzaldehydes To Access Distinct α-Carbonylnaphthalene Derivatives: C(3,4)- versus C(4,5)-Regioselectivity at Isoxazoles. *ACS Catal.* **2019**, *9*, 7328−7334. (e) Zhang, C.; Wang, G.; Zhan, L.; Yang, X.; Wang, J.; Wei, Y.; Xu, S.; Shi, M.; Zhang, J. Gold(I) or Gold(III) as Real Intermediate Species in Gold-Catalyzed Cycloaddition Reactions of Enynal/Enynone? *ACS Catal.* **2020**, *10*, 6682−6690. (f) He, Y.; Zheng, Z.; Liu, Q.; Zhang, X.; Fan, X. Solvent-Regulated Coupling of 2-Alkynylbenzaldehydes with Cyclic Amines: Selective Synthesis of Fused N-Heterocycles and Functionalized Naphthalene Derivatives. *Org. Lett.* **2020**, *22*, 9053−9058.

(12) (a) Ramachary, D. B.; Reddy, Y. V. Dienamine Catalysis: An Emerging Technology in Organic Synthesis. *Eur. J. Org. Chem.* **2012**, *2012*, 865−887. (b) Jurberg, I. D.; Chatterjee, I.; Tannert, R.; Melchiorre, P. When Asymmetric Aminocatalysis Meets the Vinylogy Principle. *Chem. Commun.* **2013**, *49*, 4869−4883. (c) Marcos, V.; Alemán, J. Old Tricks, New Dogs: Organocatalytic Dienamine Activation of α,β-Unsaturated Aldehydes. *Chem. Soc. Rev.* **2016**, *45*, 6812−6832.

(13) (a) Risley, J. M.; Van Etten, R. L. An ^{18}O Isotope Shift upon ^{13}C NMR Spectra and Its Application to the Study of Oxygen Exchange Kinetics. *J. Am. Chem. Soc.* **1979**, *101*, 252−253. (b) List, B.; Hoang, L.; Martin, H. J. New Mechanistic Studies on the Proline-Catalyzed Aldol Reaction. *Proc. Natl. Acad. Sci. U. S. A.* **2004**, *101*, 5839−5842.

(14) (a) Hariharan, P. C.; Pople, J. A. The Influence of Polarization Functions on Molecular Orbital Hydrogenation Energies. *Theor. Chim. Acta* **1973**, *28*, 213−222. (b) Becke, A. D. Density-Functional Thermochemistry. III. The Role of Exact Exchange. *J. Chem. Phys.* **1993**, *98*, 5648−5652. (c) Stephens, P. J.; Devlin, F. J.; Chabalowski, C. F.; Frisch, M. J. Ab Initio Calculation of Vibrational Absorption and Circular Dichroism Spectra Using Density Functional Force Fields. *J. Phys. Chem.* **1994**, *98*, 11623−11627. (d) Lee, C.; Yang, W.; Parr, R. G. Development of the Colle-Salvetti Correlation-Energy Formula into a Functional of the Electron Density. *Phys. Rev. B: Condens. Matter Mater. Phys.* **1988**, *37*, 785−789. (e) Marenich, A. V.; Cramer, C. J.; Truhlar, D. G. Universal Solvation Model Based on Solute Electron Density and on a Continuum Model of the Solvent Defined by the Bulk Dielectric Constant and Atomic Surface Tensions. *J. Phys. Chem. B* **2009**, *113*, 6378−6396.

(15) (a) Weigend, F.; Ahlrichs, R. Balanced Basis Sets of Split Valence, Triple Zeta Valence and Quadruple Zeta Valence Quality for H to Rn: Design and Assessment of Accuracy. *Phys. Chem. Chem. Phys.* **2005**, *7*, 3297−3305. (b) Chai, J.-D.; Head-Gordon, M. Long-Range Corrected Hybrid Density Functionals with Damped Atom-Atom Dispersion Corrections. *Phys. Chem. Chem. Phys.* **2008**, *10*, 6615−6620.

(16) (a) Frisch, M. J.; Trucks, G. W.; Schlegel, H. B.; Scuseria, G. E.; Robb, M. A.; Cheeseman, J. R.; Scalmani, G.; Barone, V.; Mennucci, B.; Petersson, G. A.; Nakatsuji, H.; Caricato, M.; Li, X.; Hratchian, H. P.; Izmaylov, A. F.; Bloino, J.; Zheng, G.; Sonnenberg,

https://doi.org/10.1021/jacs.1c03923
J. Am. Chem. Soc. 2021, 143, 8208−8220

J. L.; Hada, M.; Ehara, M.; Toyota, K.; Fukuda, R.; Hasegawa, J.; Ishida, M.; Nakajima, T.; Honda, Y.; Kitao, O.; Nakai, H.; Vreven, T.; Montgomery, J. A., Jr.; Peralta, J. E.; Ogliaro, F.; Bearpark, M.; Heyd, J. J.; Brothers, E.; Kudin, K. N.; Staroverov, V. N.; Kobayashi, R.; Normand, J.; Raghavachari, K.; Rendell, A.; Burant, J. C.; Iyengar, S. S.; Tomasi, J.; Cossi, M.; Rega, N.; Millam, J. M.; Klene, M.; Knox, J. E.; Cross, J. B.; Bakken, V.; Adamo, C.; Jaramillo, J.; Gomperts, R.; Stratmann, R. E.; Yazyev, O.; Austin, A. J.; Cammi, R.; Pomelli, C.; Ochterski, J. W.; Martin, R. L.; Morokuma, K.; Zakrzewski, V. G.; Voth, G. A.; Salvador, P.; Dannenberg, J. J.; Dapprich, S.; Daniels, A. D.; Farkas, Ö.; Foresman, J. B.; Ortiz, J. V.; Cioslowski, J.; Fox, D. J. *Gaussian 09, Revision D.01*; Gaussian, Inc.: Wallingford, CT, 2009. (b) The 3D geometries in the manuscript were generated using CYLview, 1.0b. See: Legault, C. Y. *CYLview*, 1.0b; Université de Sherbrooke: 2009; http://www.cylview.org (accessed 2021-05-11).

(17) Bertelsen, S.; Marigo, M.; Brandes, S.; Dinér, P.; Jørgensen, K. A. Dienamine Catalysis: Organocatalytic Asymmetric γ-Amination of α,β-Unsaturated Aldehydes. *J. Am. Chem. Soc.* **2006**, *128*, 12973−12980.

(18) Jensen, K. L.; Dickmeiss, G.; Jiang, H.; Albrecht, L.; Jørgensen, K. A. The Diarylprolinol Silyl Ether System: A General Organocatalyst. *Acc. Chem. Res.* **2012**, *45*, 248−264.

(19) McLeod, D.; Izzo, J. A.; Jørgensen, D. K. B.; Lauridsen, R. F.; Jørgensen, K. A. Development and Investigation of an Organocatalytic Enantioselective [10 + 2] Cycloaddition. *ACS Catal.* **2020**, *10*, 10784−10793.

(20) (a) Sit, S.-Y.; Xie, K.; Jacutin-Porte, S.; Taber, M. T.; Gulwadi, A. G.; Korpinen, C. D.; Burris, K. D.; Molski, T. F.; Ryan, E.; Xu, C.; Wong, H.; Zhu, J.; Krishnananthan, S.; Gao, Q.; Verdoorn, T.; Johnson, G. (+)-Dinapsoline: An Efficient Synthesis and Pharmacological Profile of a Novel Dopamine Agonist. *J. Med. Chem.* **2002**, *45*, 3660−3668. (b) Bonner, L. A.; Chemel, B. R.; Watts, V. J.; Nichols, D. E. Facile Synthesis of Octahydrobenzo[*h*]-isoquinolines: Novel and Highly Potent D_1 Dopamine Agonists. *Bioorg. Med. Chem.* **2010**, *18*, 6763−6770.

(21) (a) Lacoske, M. H.; Theodorakis, E. A. Spirotetronate Polyketides as Leads in Drug Discovery. *J. Nat. Prod.* **2015**, *78*, 562−575. (b) Zhang, Q.; Wang, J.; Wei, Y.; Zhai, H.; Li, Y. Stereoselective Synthesis of Spiro-2-oxabicyclo[2.2.2]octane Enabled by Ag(I)/Brønsted Acid Relay Catalysis. *Org. Lett.* **2019**, *21*, 1694−1698.

(22) (a) Bray, M. A.; Singh, S.; Han, H.; Davis, C. T.; Borgeson, B.; Hartland, C.; Kost-Alimova, M.; Gustafsdottir, S. M.; Gibson, C. C.; Carpenter, A. E. Cell Painting, a High-Content Image-Based Assay for Morphological Profiling Using Multiplexed Fluorescent Dyes. *Nat. Protoc.* **2016**, *11*, 1757−1774. (b) Svenningsen, E. B.; Poulsen, T. B. Establishing Cell Painting in a Smaller Chemical Biology Lab − A Report from the Frontier. *Bioorg. Med. Chem.* **2019**, *27*, 2609−2615.

(23) (a) Hutz, J. E.; Nelson, T.; Wu, H.; McAllister, G.; Moutsatsos, I.; Jaeger, S. A.; Bandyopadhyay, S.; Nigsch, F.; Cornett, B.; Jenkins, J. L.; Selinger, D. W. The Multidimensional Perturbation Value: A Single Metric to Measure Similarity and Activity of Treatments in High-Throughput Multidimensional Screens. *J. Biomol. Screening* **2013**, *18*, 367−377. (b) Lin, S.; Liu, H.; Svenningsen, E. B.; Wollesen, M.; Jacobsen, K. M.; Andersen, F. D.; Moyano-Villameriel, J.; Pedersen, C. N.; Nørby, P.; Tørring, T.; Poulsen, T. B. Expanding the Antibacterial Selectivity of Polyether Ionophore Antibiotics through Diversity-Focused Semisynthesis. *Nat. Chem.* **2021**, *13*, 47−55.

https://doi.org/10.1021/jacs.1c03923
J. Am. Chem. Soc. 2021, 143, 8208−8220